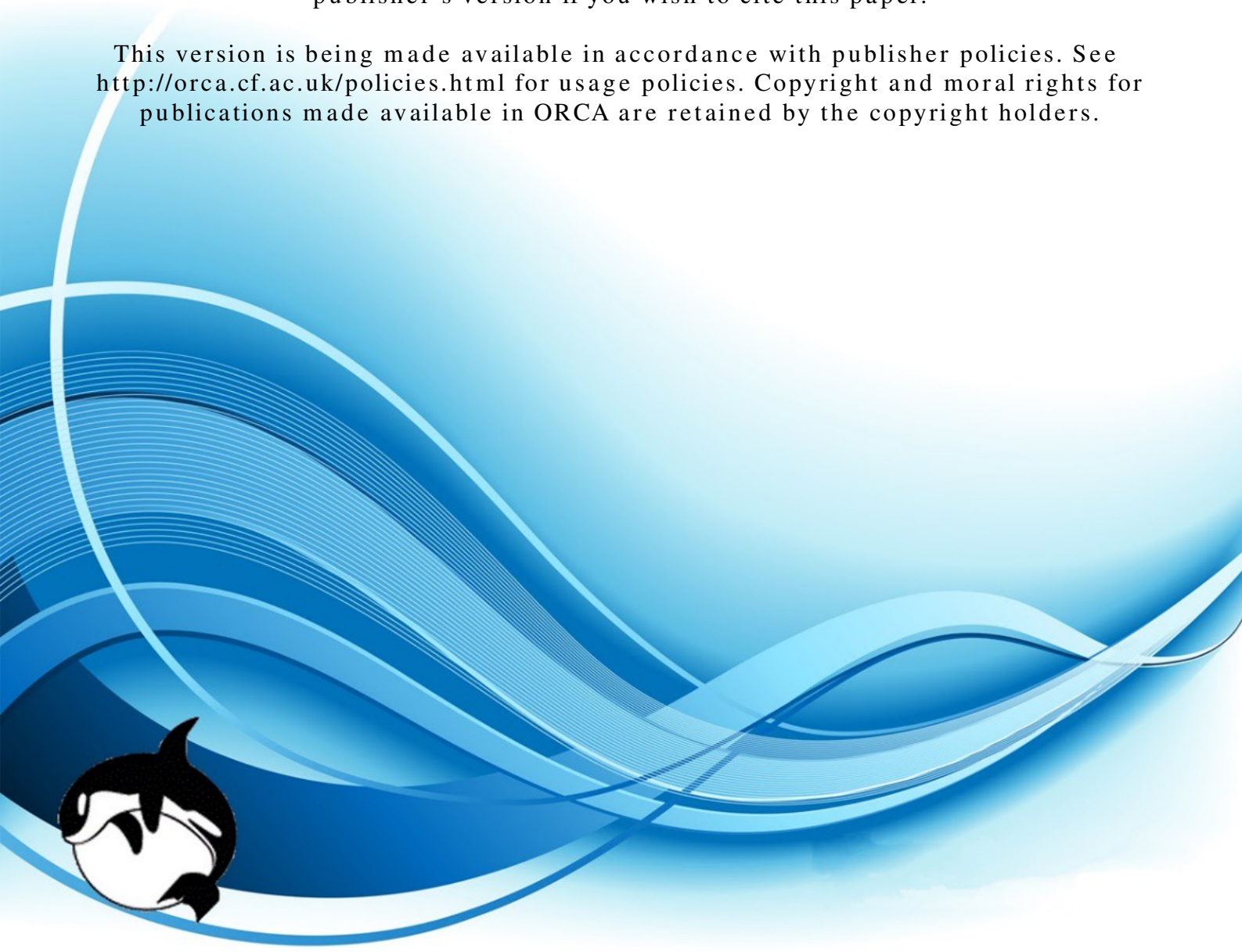

Catalysis Today 286 (2017) 147–154

Contents lists available at ScienceDirect

Catalysis Today

journal homepage: www.elsevier.com/locate/cattod

Nitrogen transfer properties in tantalum nitride based materials

Said Laassiri[a], Constantinos D. Zeinalipour-Yazdi[b], C. Richard A. Catlow[b], Justin S.J. Hargreaves[a,*]

[a] WestCHEM, School of Chemistry, Joseph Black Building, University of Glasgow, Glasgow G12 8QQ, UK
[b] Kathleen Lonsdale Materials Chemistry, Department of Chemistry, University College London, 20 Gordon Street, London WC1H 0AJ, UK

ARTICLE INFO

Article history:
Received 29 April 2016
Received in revised form 2 June 2016
Accepted 11 June 2016
Available online 5 July 2016

Keywords:
Lattice nitrogen
Tantalum nitride
Nitrogen transfer reaction

ABSTRACT

$Ta_{3-x}M_xN_y$ (M = Re, Fe, Co; x = 0, 0.25, 0.5, 1) materials with different microstructural features (*e.g.* surface area) were successfully prepared using different synthesis techniques. The dependence of nitrogen transfer properties upon tantalum nitride microstructure and its chemical composition was evaluated using the ammonia synthesis with a H_2/Ar feedstream (a reaction involving lattice nitrogen transfer). It was shown that nitrogen reactivity for tantalum nitride is more dominated by lattice nitrogen stability rather than microstructural properties. In the case of non-doped tantalum nitride, only a limited improvement of reactivity with enhanced surface area was observed which demonstrates the limited impact of microstructure upon reactivity. However, the nature of the transition metal dopant as well as its content was observed to play a key role in the nitrogen transfer properties of tantalum nitride and to impact strongly upon its reactivity. In fact, doping tantalum nitride with low levels of Co resulted in enhanced reactivity at lower temperature.

1. Introduction

Nitrogen is of central importance in many industrial processes with nitrogen containing compounds being used in numerous commercial products including synthetic fertilizers, dyes, explosives, and resins [1]. Moreover, nitrogen is an essential component of proteins and thus is an important nutritional element [2]. Molecular nitrogen is relatively inert and the preparation of almost all nitrogen containing products requires the use of combined nitrogen such as HCN, HNO_3, $CO(NH_2)_2$, or simply NH_3 as an activated nitrogen building block. Behind this apparent diversity of precursor, NH_3 is used directly in the Andrussow Process to make HCN [3] and in the Ostwald Process to make HNO_3 [4] for example. However, in view of the energy intensive nature of industrial ammonia synthesis process, its large scale utilisation as a direct/indirect activated nitrogen building block incurs considerable economic and environmental costs [5]. The catalytic process of ammonia generation from dinitrogen and dihydrogen requires high pressure and moderate temperature operation to ensure acceptable industrial synthesis rates. The overall process consumes 1–2% of the world's annual energy production and requires significant quantities of natural gas for feedstock synthesis. Therefore, the necessity for developing new efficient routes for more direct nitrogen transfer/fixation reactions is an area of great interest which could have wide ranging impact.

Different approaches have been proposed for alternative pathways for nitrogen fixation including dinitrogen reduction to ammonia at ambient pressure using transition metal centres from nitrogenase in the liquid phase [6,7], electrochemical NH_3 generation [8–10] and dinitrogen photoreduction to ammonia [11–13]. However, numerous scientific challenges and technological issues need to be solved prior to practical use of these systems. In principle, the reactivity of lattice nitrogen of nitride materials towards dihydrogen to yield ammonia or towards more complex molecules (*e.g.* CH_4, MeOH) to yield nitrogen containing products constitutes a simple and novel pathway for developing a new generation of materials for nitrogen fixation reactions. Nitrogen mobility within binary and ternary nitride structures and their nitrogen transfer abilities have motivated several studies. For instance, Alexander et al. studied the ability of a number of binary nitrides to be reduced using dihydrogen to yield ammonia [14,15]. Ternary cobalt molybdenum nitride was also reported for his high nitrogen mobility and its ability to be reduced from Co_3Mo_3N to Co_6Mo_6N with H_2 to generate ammonia [16]. The hydrolysis of nitride materials has also been investigated as a means for solar ammonia production [17,18]. In this approach the ammonia synthesis reaction was separated into two different steps: (i) the metal nitride is obtained by dinitrogen reduction at high temperature and (ii) the metal nitride is subsequently hydrolysed to yield ammonia. Related to this concept Mg_3N_2 has been used as an *in-situ* source of ammonia in the

* Corresponding author.
E-mail address: Justin.Hargreaves@glasgow.ac.uk (J.S.J. Hargreaves).

http://dx.doi.org/10.1016/j.cattod.2016.06.035

Table 1
Structural and textural properties of tantalum nitride related materials.

Samples	Nitridation conditions		S_{BET}[a]/m^2 g^{-1}	Phase composition/XRD	Nitrogen content[b]/wt.%
	Precursor	Ammonolysis			
C-Ta_3N_5	Crystalline Ta_2O_5	T = 900 °C for 9h	10	019–1291	11.28 (11.42)[c]
A-Ta_3N_5	Amorphous Ta_2O_5	T = 750 °C for 9h	50	019–1291	10.99
$Ta_{2.5}Re_{0.5}N_y$	Co-precipitate	T = 750 °C for 9h	10	019–1291	7.93
$Ta_{2.5}Fe_{0.5}N_y$	Co-precipitate	T = 750 °C for 9h	13	019–1291	5.54
$Ta_{2.75}Co_{0.25}N_y$	Co-precipitate	T = 750 °C for 9h	27	019–1291	5.12
$Ta_{2.5}Co_{0.5}N_y$	Co-precipitate	T = 750 °C for 9h	23	019–1291	8.54
$Ta_2Co_1N_y$	Co-precipitate	T = 750 °C for 9h	15	019–1291	6.11

[a] S_{BET} is the specific surface area evaluated using the BET model.
[b] nitrogen analysis undertaken using an Exeter Analytical CE-440 Elemental Analyser.
[c] Stoichiometric nitrogen content corresponding to phase pureTa_3N_5.

transformation of esters to primary amides in the presence of protic solvents [19,20]. In all these examples, nitride materials acted as a source of reactive nitrogen that can directly undergo reaction through mechanisms analogous to the Mars-van Krevelen (MvK) one, which is a current area of interest for both catalytic [21] and electrocatalytic [22] ammonia synthesis using nitride catalysts. If the regeneration of nitrogen depleted phases during reaction was realisable using dinitrogen directly, materials operating through processes akin to the MvK mechanism could be considered as means to by-pass the use of activated nitrogen building blocks such as ammonia itself in multistage processes. These routes would use the lattice nitrogen component as the source of pre-activated reactant.

In this context, tantalum nitride presents potential for developing very active nitrogen transfer materials. Ta_3N_5 is composed of irregular TaN_6 octahedra with both three and four coordinate nitrogen atoms and has the pseudobrookite (Fe_2TiO_5) structure [23,24]. The lattice nitrogen was found to be thermochemically labile and reactive to hydrogen to generate ammonia under reducing conditions [15]. Thus, Ta_3N_5 could be considered as reservoir of activated nitrogen species. In such a scheme, the reactivity might be controlled by lattice nitrogen mobility. Therefore, controlling the nitrogen mobility in tantalum nitride materials could be the key for developing highly active materials. In materials operating via mechanisms akin to MvK, lattice component mobility has been found to be dependent upon: (i) textural and structural properties [25], (ii) chemical composition [26] or a combination of both. In an analogous manner, the nitrogen transfer properties of Ta_3N_5 are expected to depend upon structural and textural properties i.e. surface area, and the reactivity of tantalum nitride "lattice N" under reaction conditions.

In this work we have explored the possibility to alter the reactivity of Ta_3N_5 by: (i) modification of the structural and textural properties of Ta_3N_5, (ii) alteration of the reactivity of tantalum nitride lattice nitrogen by doping with transition metals. For this, a series of $Ta_{3-x}M_xN_y$ (M = Re, Co, Fe) nitrides were prepared by high temperature ammonolysis of various precursors and their behaviour characterised.

2. Experimental section

2.1. Material synthesis

2.1.1. Preparation of Ta_3N_5 materials

Different approaches to the preparation of Ta_3N_5 have been adopted.

(I) Ammonolysis of crystalline tantalum oxide precursor: Ta_3N_5 was prepared by ammonolysis of crystalline Ta_2O_5 (Sigma Aldrich, 99%) under NH_3 (BOC, 99.98%) atmosphere at a flow rate of 60 ml min^{-1} at different nitridation temperatures as discussed later on. This material is labelled C-Ta_3N_5.

(II) Ammonolysis of amorphous tantalum oxide precursor: Ta_3N_5 was prepared by ammonolysis of an amorphous tantalum oxide precursor. Amorphous tantalum oxide was prepared by precipitation of $TaCl_5$, dissolved in ethanol, using ammonia as a precipitating agent [27]. Subsequently, the amorphous precursor was subjected to an ammonolysis step under NH_3 (BOC, 99.98%) gas at a flow rate of 60 ml min^{-1} at 750 °C (Table 1). The material is labelled A-Ta_3N_5.

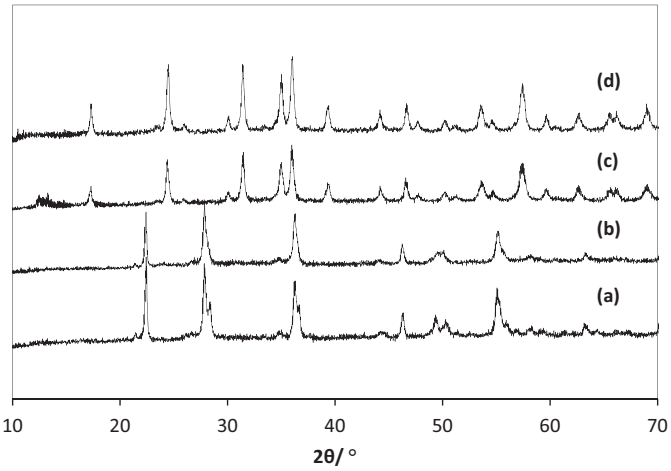

Fig. 1. X-ray diffraction patterns collected after the ammonolysis of crystalline Ta_2O_5. (a) Ta_2O_5, (b) ammonolysis T = 700 °C (c) ammonolysis T = 800 °C (d) ammonolysis T = 900 °C.

2.1.2. Preparation of doped $Ta_{3-x}M_xN_y$ (M = Re, Fe, Co and x = 0.5)

Doped tantalum materials were prepared by ammonolysis of co-precipitated $TaCl_5$ and transition metal precursors. In summary, appropriate amounts of $TaCl_5$ and metal precursors were dissolved in ethanol and then precipitated with a large excess of ammonia. The precipitate was collected by filtration, washed with ethanol and water several times and then after dried at 100 °C for 12 h. The as-prepared materials were then subjected to an ammonolysis step at 750 °C for 9 h.

2.2. Physical and textural characterization

2.2.1. Elemental analysis

Nitrogen analysis was undertaken using total combustion using an Exeter Analytical CE-440 Elemental Analyser.

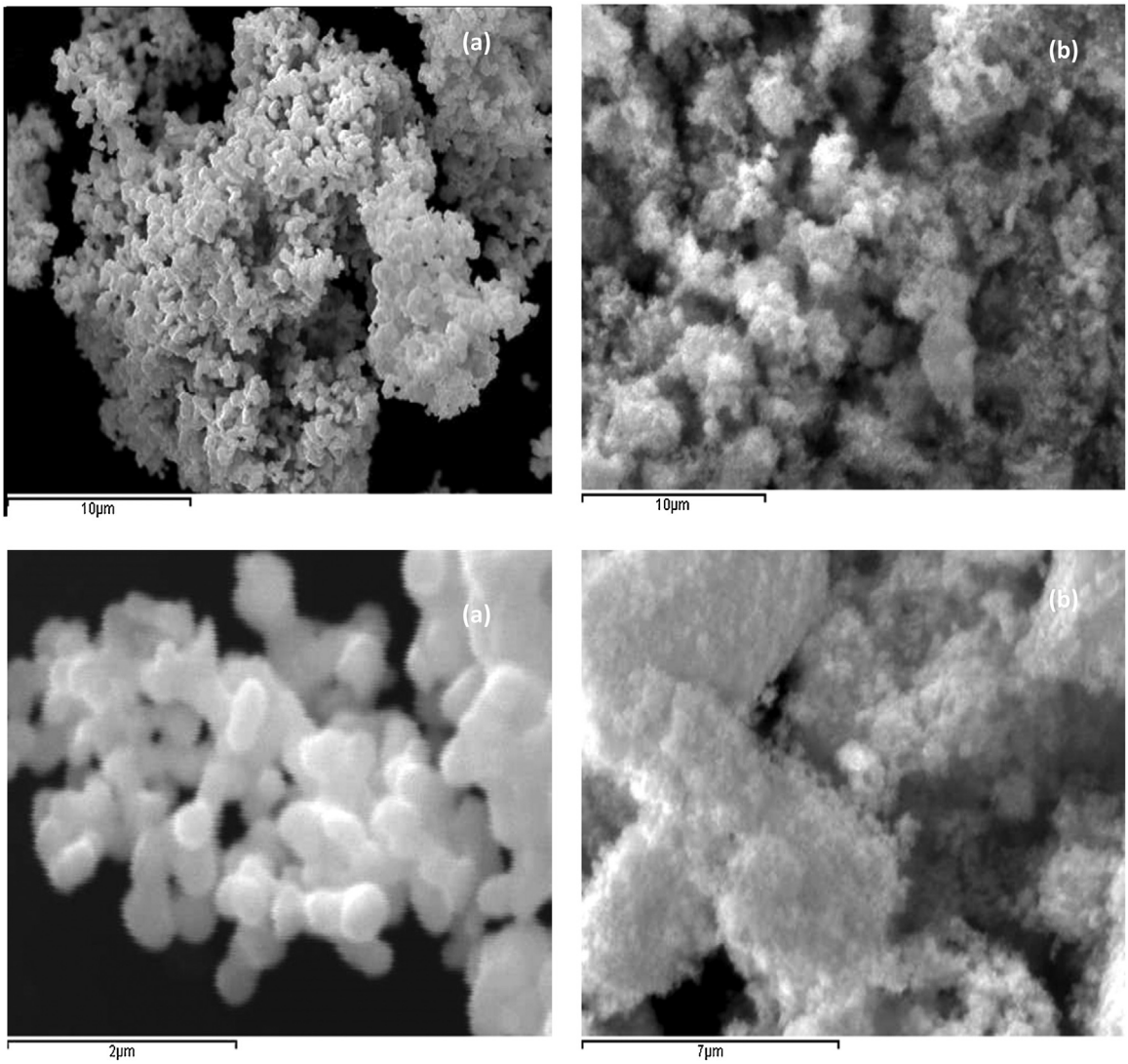

Fig. 2. SEM micrographs of (a) C-Ta_3N_5, (b) A- Ta_3N_5.

2.2.2. X-ray diffraction

Diffraction patterns were collected on a Siemens D5000 instrument, using Cu Kα radiation (λ = 0.154 nm) as X-ray source. A 2θ range between 10° and 80° was scanned applying a step size of 0.02° and a counting rate of 1 s per step. Phase identification was undertaken by comparison with PDF database files.

2.2.3. Surface area measurement

Surface areas were obtained by application of the BET method from N_2 physisorption isotherms determined at −196 °C. Prior to measurement, a known mass of sample was degassed *in vacuo* at 300 °C for 5 h.

2.2.4. Scanning electron microscopy

Scanning electron microscopy was performed on Philips XLSE-Mand FEI Quanta 200 F Environmental instruments operating at 20 kV.

2.3. Nitrogen transfer properties

Nitrogen transfer properties of Ta_3N_5 and $Ta_{3-x}M_xN_y$ materials were evaluated using the ammonia synthesis reaction as a model reaction to assess the reactivity of lattice nitrogen.

In a typical reaction test, 0.3 g of material was placed in the reactor and was pre-treated for 2 h under a 25 vol% H_2 in N_2 gas mixture (flow rate = 60 ml min^{-1}; T = 700 °C). The reaction was then performed under a flow composed either of 25 vol% H_2 in N_2 or 25 vol% H_2 in Ar at a total gas feed of 60 ml min^{-1}. Ammonia production was determined by measurement of the decrease in conductivity of 200 ml of a 0.00108 M H_2SO_4 solution through which the reactor effluent stream was flowed.

3. Results and discussion

3.1. Evolution of the structural and textural properties with synthesis method

The evolution of Ta_2O_5 structural properties during nitridation of the different precursors was monitored by the XRD and SEM analyses presented in Figs. 1–3 . Table 1 summarises the structural and textural features of the prepared nitrides as a function of the experimental synthesis conditions.

3.1.1. Ammonolysis of crystalline tantalum oxide precursor

Structural transformation of tantalum oxide after the ammonolysis step at temperatures ranging between 700 and 900 °C was followed by XRD (Fig. 1).

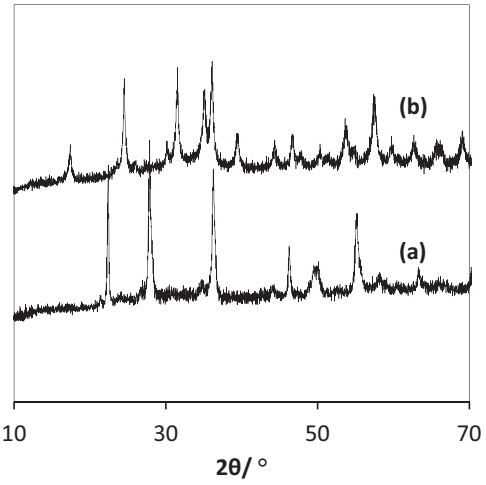

Fig. 3. XRD patterns collected after the ammonolysis step of (a) crystalline Ta_2O_5, (b) amorphous Ta_2O_5 at 750 °C for 9 h.

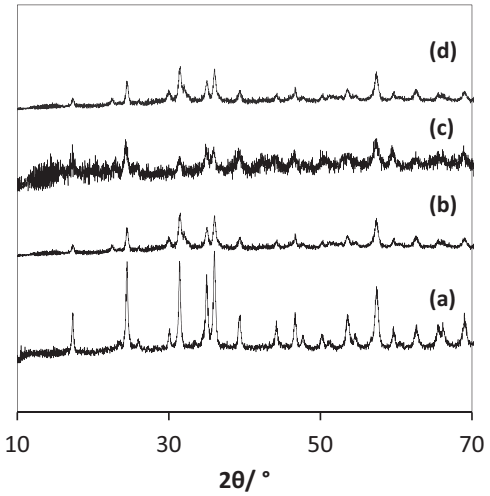

Fig. 4. XRD patterns collected after the ammonolysis step of (a) C-Ta_2O_5, (b) $Ta_{2.5}Fe_{0.5}N_y$, (c) $Ta_{2.5}Co_{0.5}N_y$, (d) $Ta_{2.5}Re_{0.5}N_y$.

The phase of the starting precursor was verified and all observed reflections corresponded to orthorhombic Ta_2O_5 (Fig. 1a). At low nitridation temperature, T = 700 °C, no change in the crystalline structure was observed and only Ta_2O_5 was detected (Fig. 1b). At higher nitridation temperature, T ≥ 800 °C, all detected reflections matched to Ta_3N_5 (PDF number: 019-1291) indicating the successful preparation of Ta_3N_5. However, complete transformation with nitrogen contents (11.28 N wt.%) close to the stoichiometric value (11.42 N wt.%) only occurred at 900 °C (Table 1, Fig. 1d). Since Ta_3N_5 can be decomposed into TaN at high temperature, it is interesting to note that no additional phases were evident. The intense and relatively narrow reflections correspond to a well ordered phase comprising large coherent diffraction domains and the sharpness of the XRD reflections reflect the effect of sintering during nitridation. SEM images (Fig. 2a) confirmed the presence of large particles of Ta_3N_5 as consistent with the low surface area of C-Ta_3N_5 (~10 $m^2\ g^{-1}$).

3.1.2. Ammonolysis of amorphous tantalum oxide precursor

To address the low surface area of Ta_3N_5 when prepared from crystalline Ta_2O_5, preparation of Ta_3N_5 from an amorphous tantalum oxide precursor was also investigated. XRD patterns collected after ammonolysis of crystalline Ta_2O_5 and amorphous Ta_2O_5 at 750 °C are presented in Fig. 3. When crystalline Ta_2O_5 is used as precursor, no changes upon ammonolysis were observed by XRD analysis (Fig. 2a). However, when amorphous tantalum oxide was used as precursor, the Ta_3N_5 phase was formed at temperatures as low as 750 °C (Fig. 3b, Table 1). For A-Ta_3N_5, XRD patterns (Fig. 3b) showed only reflections corresponding to Ta_3N_5 (PDF number: 019-1291) suggesting the preparation of pure Ta_3N_5 phase. Furthermore, nitrogen content evaluated by CHN analysis was 10.99 wt.% which is consistent with the theoretical value 11.42 wt.% for Ta_3N_5. Compared to the case of C-Ta_2O_5 discussed above, broader XRD reflections were observed (Fig. 3) suggesting a less ordered/less crystalline material. As result of lowering the nitridation temperature, A-Ta_3N_5 possesses a higher surface area of ~50 $m^2\ g^{-1}$ compared to that for C-Ta_3N_5 which was ~10 $m^2\ g^{-1}$.

3.1.3. Preparation of doped $Ta_{3-x}M_xN_y$

$Ta_{3-x}M_xN_y$ (M = Re, Fe, Co and x = 0.5). Doped tantalum materials were prepared using a similar procedure to A-Ta_3N_5. First, amorphous precursors were prepared by co-precipitation. Then, the nitride phase was obtained by an ammonolysis step at 750 °C for 9 h. XRD patterns recorded for $Ta_{3-x}M_xN_y$ (M = Re, Fe, Co and x = 0.5) are presented in Fig. 4. For all materials, only phases related to Ta_3N_5 (PDF number: 019-1291) are observed, and no characteristic reflections related to other transition metal nitride or oxides were detected. However, it should be noted that some reflections of such metal nitrides, as in case of cobalt nitride, would overlap with the tantalum nitride reflections [28]. Moreover, no obvious shifts for the XRD reflections at a doping level x = 0.5 as may have been anticipated had incorporation of dopants into the Ta_3N_5 structure occurred.

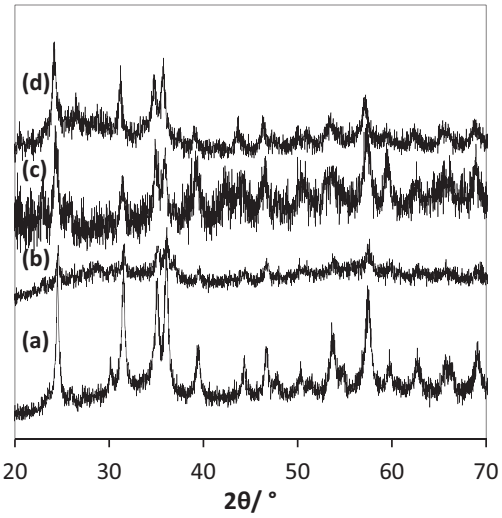

Fig. 5. XRD patterns collected after the ammonolysis step of (a) C-Ta_2O_5, (b) $Ta_{2.75}Co_{0.25}N_y$, (c) $Ta_{2.5}Co_{0.5}N_y$, (d) Ta_2CoN_y.

The effect of such metal doping was more obvious on the textural properties of Ta_3N_5 since a significant decrease of the surface area of $Ta_{3-x}M_xN_y$ (M = Re, Fe, Co and x = 0.5) was observed upon metal doping (Table 1). Doped tantalum materials also showed lower nitrogen content than the corresponding Ta_3N_5 material, although it has to be borne in mind that this could relate to a greater sensitivity of the materials towards oxidation upon discharge from the reactor and exposure to air.

$Ta_{3-x}Co_xN_y$ (x = 0.25, 0.5, and 1). $Ta_{3-x}Co_xN_{5-y}$ materials were prepared at different cobalt concentration, x = 0.25, 0.5, and 1, to investigate the effect of the concentration of cobalt on lattice nitrogen mobility. XRD patterns recorded for $Ta_{3-x}Co_xN_y$ materials are presented in Fig. 5. Only phases related to Ta_3N_5 (PDF number: 019-1291) were observed by XRD. However when compared to A-Ta_3N_5,

Table 2
Summary of nitrogen transfer properties in C-Ta_3N_5.

	Total N content/wt%		Ammonia production[a]/μmol
	Pre-reaction	Post-reaction	
H_2:Ar	11.28	6.71	325
H_2:N_2	11.28	6.22	441

Initial N content corresponding to 0.3 g C-Ta_3N_5 = 2417 μmol.
[a] Cumulative ammonia production after 9 h on stream.

XRD reflections of $Ta_{3-x}Co_xN_y$ were of lower intensity suggesting the material to be less crystalline. Careful inspection of the XRD patterns does not evidence any shifts in the position of reflections up to x = 0.5, indicating there to be no change in lattice parameter. Nevertheless, a higher cobalt concentration, x = 1, results in a peak position shift to lower 2θ. Varying the degree of cobalt concentration also affected the surface area and nitrogen content of $Ta_{3-x}Co_xN_y$. A gradual decrease in the surface area of $Ta_{3-x}Co_xN_y$ was observed with the increase of Co concentration, while nitrogen content was maximal for the $Ta_{2.5}Co_{0.5}N_y$ composition and decreased at x = 1 (Table 1).

3.2. Reactivity of Ta_3N_5 related material for ammonia generation

3.2.1. Reactivity of non-doped Ta_3N_5

C-Ta_3N_5. The ammonia synthesis reaction, at different reaction temperatures and gas atmospheres, was conducted on C-Ta_3N_5 to provide an initial general overview of tantalum nitride reactivity to dihydrogen (Table 2, Fig. 6).

The production of ammonia, using 60 ml min^{-1} flow of a 1:3 Ar:H_2 mixture at different temperatures is presented Fig. 6A. At low temperature region T ≤ 500 °C, only a very limited amount of ammonia is produced. Nevertheless, the ammonia yield was observed to increase significantly at T ≥ 600 °C and a cumulative production of ammonia of ca 325 μmol was measured at the end of reaction after 9 h on stream. Furthermore, the post-reaction nitrogen content was found to be 6.71 wt.% confirming the consumption of lattice N. Ammonia synthesis was also studied using 60 ml min^{-1} of a 1:3 N_2:H_2 mixture (Fig. 6B). Ta_3N_5 behaved in a similar manner to the case with the Ar/H_2 feed. Ammonia production was only observed at high temperature T ≥ 600 °C and resulted in clear nitrogen content reduction (Table 2). In both atmospheres, post-reaction XRD analysis confirmed that C-Ta_3N_5 structure was maintained despite the significant reduction in N content during reactivity tests (Fig. 7, Table 2), suggesting that N-containing X-ray amorphous components may be important in this regard.

A-Ta_3N_5. In order to evaluate the effect of the textural properties and structural properties of A-Ta_3N_5 with respect to C-Ta_3N_5, a reactivity test with 60 ml min^{-1} flow of a 1:3 Ar: H_2 feed at a relatively low reaction temperature was undertaken. Ammonia production as a function of reaction time at 500 °C is presented in Fig. 8. Despite the enhanced surface area of A-Ta_3N_5 (~50 m^2 g^{-1}) only a limited amount of ammonia was produced ~49 μmol NH_3 against ~12 μmol NH_3 for C-Ta_3N_5. The limited improvement of tantalum nitride reactivity with enhanced textural and structural properties demonstrates the limited impact of microstructure upon reactivity.

3.2.2. Impact of chemical composition on tantalum nitride reactivity

$Ta_{3-x}M_xN_y$ (M = Re, Fe, Co and x = 0.5)

A series of $Ta_{3-x}M_xN_y$ (M = Re, Fe, Co and x = 0.5) nitrides were prepared and studied for the ammonia synthesis reaction (Table 3, Fig. 9). Depending on the nature of the dopant, tantalum nitride reactivity was either enhanced or diminished. Upon Re and Fe doping, ammonia synthesis is inhibited at lower temperatures. In both materials ammonia generation occurred only during the first two hours of reaction before it ceased and a very limited amount of ammonia was produced (<40 NH_3 μmol for both materials). In spite of Re and Fe being reported as active catalysts for ammonia production (*e.g.* promoted Fe[29,30], $CoRe_4$ [31,32]) no enhancement of tantalum nitride reactivity was observed. CHN analysis confirmed

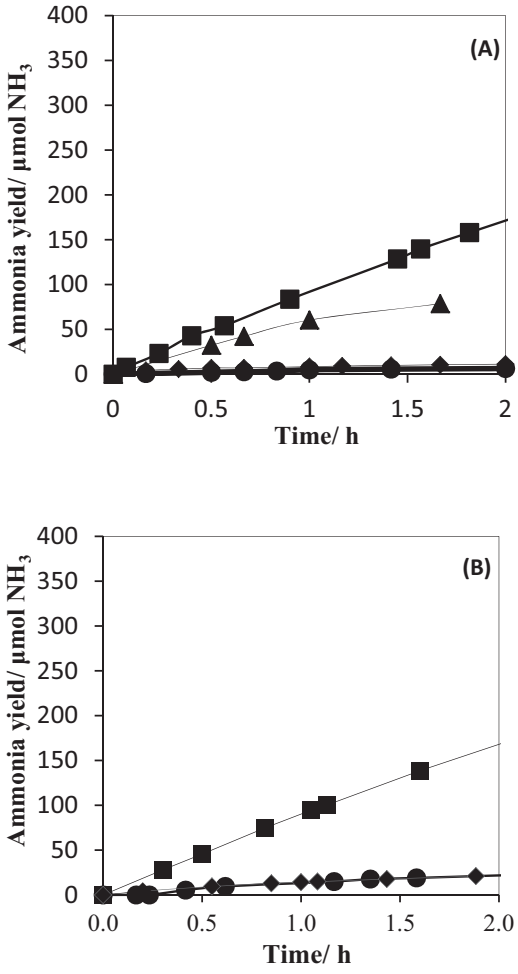

Fig. 6. Ammonia yield resulting from C-Ta_3N_5 reduction: as a function of temperature (■: 700 °C, ▲600 °C, ● 500 °C, ♦ 400 °C) under (A) 3:1 H_2:Ar, (B) 60 ml 3:1 H_2:N_2 gas mixture.

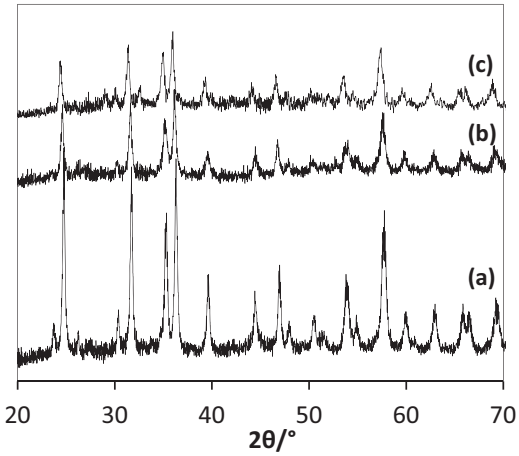

Fig. 7. XRD diffraction patterns collected for (a) C-Ta_3N_5 pre-reaction, (b) Ta_3N_5 post-reaction under N_2: H_2 and (c) Ta_3N_5 post-reaction under Ar: H_2.

Table 3
Summary of nitrogen transfer properties of tantalum nitride related structures after 5 h reaction under 60 ml min^{-1} of 1:3 Ar: H_2.

Samples	Nitrogen content/wt.%		Total N content/μmol/0.3 g of material	NH_3 produced/μmol	% lattice N lost converted to NH_3
	Pre- reaction	Post- reaction			
$Ta_{2.5}Re_{0.5}N_y$	7.93	5.09	1699	35	6
$Ta_{2.5}Fe_{0.5}N_y$	5.54	3.84	1187	38	10
$Ta_{2.5}Co_{0.5}N_y$	8.54	3.04[a]	1830	380 (950[a])	81[a]

[a] Value obtained after 24 h of reaction.

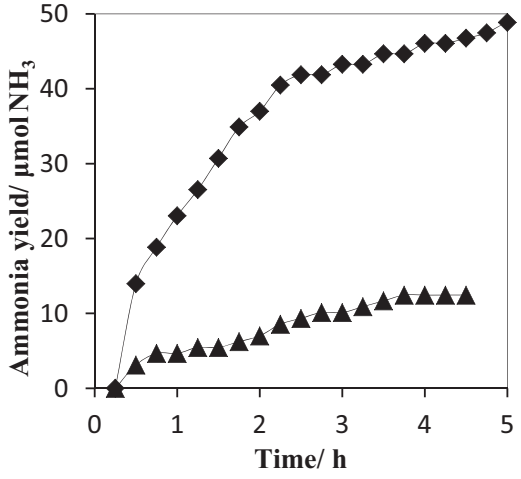

Fig. 8. Ammonia yield for Ta_3N_5 reduction with 60 ml min^{-1} of 1:3 Ar:H_2 at T = 500 °C: ▲ C-Ta_3N_5, ♦ A-Ta_3N_5.

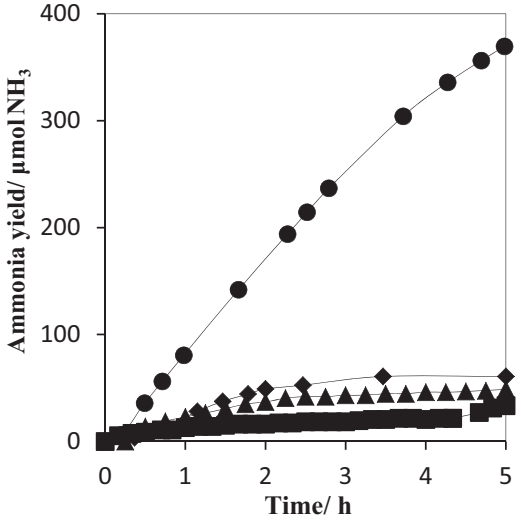

Fig. 9. Ammonia yield of $Ta_{2.5}M_{0.5}N_{5-y}$ reduction with 60 ml min^{-1} flow of a 1:3 Ar:. H_2 at 500 °C: (▲) A-Ta_3N_5, (■) $Ta_{2.5}Fe_{0.5}N_y$, (●) $Ta_{2.5}Co_{0.5}N_y$, (♦) $Ta_{2.5}Re_{0.5}N_y$

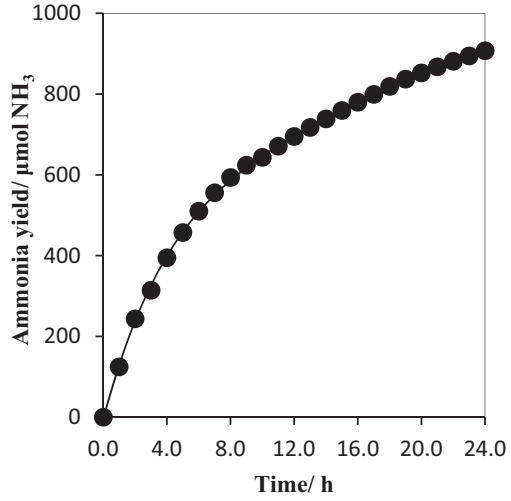

Fig. 10. Ammonia yield of $Ta_{2.5}Co_{0.5}N_y$ at 500 °C using 60 ml min^{-1} 1:3 Ar: H_2 feed gas.

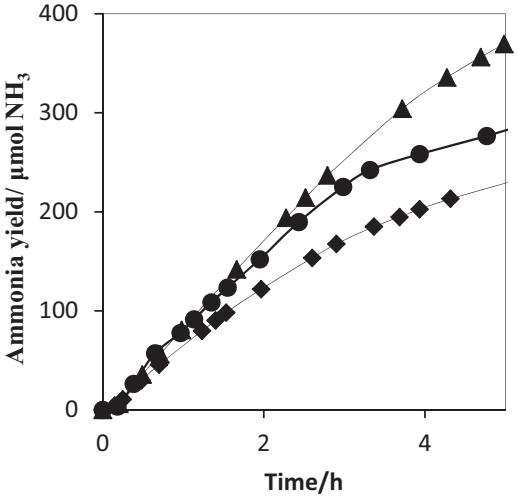

Fig. 11. Yield of ammonia $Ta_{3-x}Co_xN_{5-y}$ reduction with 60 ml min^{-1} flow of a 1:3. Ar: H_2 at 500 °C: (▲)$Ta_{2.5}Co_{0.5}N_y$, (●) $Ta_{2.75}Co_{0.25}N_y$, (♦) $Ta_{2.5}Re_{0.5}N_y$

N- loss in both materials as a result of reaction (Table 3). This suggests that doping Ta_3N_5 with Re or Fe enhances the loss of lattice nitrogen as N_2 rather than the reaction of lattice N- with H_2 to yield NH_3. In contrast, nitrogen transfer properties are considerably enhanced when Co was used as doping metal. ~380 NH_3 μmol of ammonia is generated during the first 5 h of reaction and a total ~950 NH_3 μmol was generated after 24 h (Fig. 10). The amount of ammonia generated at the end of reaction corresponds to the reaction of 52% the total available lattice nitrogen with hydrogen. Post reaction CHN analysis confirmed the reduction of N- content in $Ta_{2.5}Co_{0.5}N_y$ to 3.04 wt.%. Thus, almost 80% of N- lost during the reaction reacted to H_2 to produce ammonia (Table 3). Since the presence of cobalt nitride can't be excluded from the XRD results, cobalt nitride decomposition could be invoked to explain ammonia synthesis at low temperature. However, cobalt nitride decomposition is reported to start at temperatures as low as 250 °C with rapid reduction to metallic Co. Thus, Co complete reduction would be expected to occur during the pre-treatment step. Therefore, the $Ta_{2.5}Co_{0.5}N_y$ improved reactivity at low temperature is suggested to be a direct modification upon the reactivity of the Ta-N system due to the presence of Co.

$Ta_{3-x}Co_xN_y$ (x = 0.25, 0.5, 1). $Ta_{3-x}Co_xN_y$ materials with different concentrations of cobalt, x = 0.25, 0.5, 1, were prepared and tested

Table 4
Summary of nitrogen transfer properties of $Ta_{3-x}Co_xN_y$ (x = 0.25, 0.5, 1) using 60 ml min^{-1} flow of 1:3 Ar: H_2 feed gas.

	Nitrogen content/wt.%		Total N content/μmol/0.3 g of material	NH_3 produced after 5 h/μmol	% lattice N lost converted to NH_3
	Pre- reaction	Post- reaction			
$Ta_{2.75}Co_{0.25}N_{5-y}$	5.12	4.60	1097	231	47
$Ta_{2.5}Co_{0.5}N_{5-y}$	8.54	3.04[a]	1830	380 (950[a])	81[a]
$Ta_2Co_1N_{5-y}$	6.11	2.71	1309	173	24

[a] Value obtained after 24 h of reaction.

for ammonia synthesis. The results are presented in Fig. 11 and Table 4.

At low levels of doping, $Ta_{2.75}Co_{0.25}N_{5-y}$ presents enhanced reactivity in respect to non-doped materials (C-Ta_3N_5 and A-Ta_3N_5). Post reaction CHN analysis indicates that ammonia production was accompanied by nitrogen lattice reduction to 4.6 wt.% and that 47% of nitrogen lost during reaction was reactive to hydrogen to generate ammonia. At x = 0.5, ammonia generation is only slightly enhanced with Co concentration. Nevertheless 81% of lost lattice nitrogen is found to be reactive to hydrogen. Further Co doping resulted in a less reactive material and lower ammonia generation was observed. Post-reaction analysis revealed a considerable nitrogen lattice reduction lost as dinitrogen and that only 24% of lost lattice nitrogen reacted to hydrogen. The presence of additional cobalt that can act as active centre for nitrogen lattice depletion could explain the significant nitrogen lattice loss in $Ta_2Co_1N_y$.

3.3. Nitrogen bulk transfer properties on Ta_3N_5 related materials

The dependence of nitrogen transfer properties upon microstructure (crystalline phase, surface area) and chemical composition (transition metal dopant nature) was evaluated using ammonia synthesis (a reaction involving lattice nitrogen transfer). Improved reactivity was found in the cobalt doped system and interestingly, this cannot be explained solely on the basis of microstructure since the surface area of these materials are intermediate between those of the dopant-free C-Ta_3N_5 and A-Ta_3N_5 materials. In view of post-reaction analysis results (CHN analysis, XRD), ammonia synthesis in the presence or absence of dinitrogen proceeds through routes akin to the Mars – van Krevelen mechanism in which lattice nitrogen is the active species. Thus, the amount of ammonia produced during reactivity test can be used as an indirect measure of tantalum lattice nitrogen transfer properties, through the following process:

$$Ta_3N_5 + 3/2\delta H_2 \rightarrow Ta_3N_{5-\delta} + \delta NH_3$$

In the non-doped Ta_3N_5 system, nitrogen has been confirmed to be labile and reactive towards hydrogen to generate ammonia. Unfortunately, nitrogen lattice reactivity of C-Ta_3N_5 and A-Ta_3N_5 was only observed at high temperature. The limited improvement of nitrogen reactivity of A-Ta_3N_5 is more dominated by lattice nitrogen stability than by microstructural properties.

Doping tantalum nitride with transition metals seemingly may provide a route to alter lattice N- stability either directly or through modified dihydrogen activation and could provide a more direct approach to tailor its nitrogen transfer properties. Doping tantalum nitride structure by Fe and Re did alter tantalum lattice N-stability at low temperature. However, almost 90% of lattice nitrogen was depleted as dinitrogen possibly reflecting the efficacy of the dopants in ammonia decomposition. Doping tantalum nitride with low levels of Co proved to be the most appropriate way to achieve higher reactivity at lower temperature to yield ammonia. Since, ammonia synthesis reaction proceeds through a Mars – van Krevelen related mechanism with consumption of nitrogen from the solid, the higher reactivity of $Ta_{2.5}Co_{0.5}N_5$ can be attributed to a higher nitrogen transfer properties of cobalt doped tantalum nitride structure.

4. Conclusion

In this work, $Ta_{3-x}M_xN_y$ (M = Re, Fe, Co; x = 0, 0.25, 0.5, 1) materials with different microstructural features were prepared using classical synthesis by ammonolysis at high temperature and by soft chemistry synthesis techniques. Due to the high surface area of material prepared using soft chemistry processes, the impact of microstructure on the nitrogen reactivity under hydrogen was determined. It was clearly demonstrated that the nitrogen transfer properties of these materials does not directly depend on the accessible surface area. As ammonia synthesis on tantalum nitride materials proceeds through a pathway akin to the Mars van-Krevelen mechanism, the availability of active nitrogen species on the material surface was found to be the key to tailor its reactivity. Doping tantalum nitride with transition metals provided a direct way to modify the loss of nitrogen under dihydrogen atmosphere. Doping tantalum nitride with low levels of Co proved to be the most appropriate way to achieve higher reactivity at lower temperature to yield ammonia.

Acknowledgements

We are grateful to Mrs Kim Wilson for very kindly conducting the nitrogen elemental analyses. We also wish to express our appreciation to the Engineering and Physical Sciences Research Council through the generous provision of funding through grants EP/L02537X/1 and EP/L026317/1.

References

[1] J.N. Galloway, A.R. Townsend, J.W. Erisman, M. Bekunda, Z. Cai, J.R. Freney, L.A. Martinelli, S.P. Seitzinger, M.A. Sutton, Science 320 (2008) 889.
[2] J.N. Galloway, E.B. Cowling, AMBIO: J. Hum. Environ. 31 (2002) 64.
[3] L. Andrussow, Angew. Chem. 48 (1935) 593.
[4] Improvements Manuf. Nitric Acid Nitrogen Oxides, 1902, GB Patent, 190200698.
[5] Y. Tanabe, Y. Nishibayashi, Coord. Chem. Rev. 257 (2013) 2551.
[6] D.V. Yandulov, R.R. Schrock, Science 301 (2003) 76.
[7] F. Simpson, R. Burris, Science 224 (1984) 1095.
[8] V. Kordali, G. Kyriacou, C. Lambrou, Chem. Commun. (2000) 1673.
[9] E. Skulason, T. Bligaard, S. Gudmundsdottir, F. Studt, J. Rossmeisl, F. Abild-Pedersen, T. Vegge, H. Jonsson, J.K. Norskov, Phys. Chem. Chem. Phys. 14 (2012) 1235.
[10] I.A. Amar, C.T.G. Petit, R. Lan, G. Mann, S. Tao, RSC Adv. 4 (2014) 18749.
[11] D. Zhu, L. Zhang, R.E. Ruther, R.J. Hamers, Nat. Mater. 12 (2013) 836.
[12] J.R. Christianson, D. Zhu, R.J. Hamers, J.R. Schmidt, J. Phys. Chem. B 118 (2014) 195.
[13] J. Soria, J.C. Conesa, V. Augugliaro, L. Palmisano, M. Schiavello, A. Sclafani, J. Phys. Chem. 95 (1991) 274.
[14] A.M. Alexander, J.S.J. Hargreaves, C. Mitchell, Top. Catal. 56 (2013) 1963.
[15] A.M. Alexander, J.S.J. Hargreaves, C. Mitchell, Top. Catal. 55 (2012) 1046.
[16] S.M. Hunter, D.H. Gregory, J.S.J. Hargreaves, M. Richard, D. Duprez, N. Bion, ACS Catal. 3 (2013) 1719.
[17] R. Michalsky, A.M. Avram, B.A. Peterson, P.H. Pfromm, A.A. Peterson, Chem. Sci. 6 (2015) 3965.
[18] R. Michalsky, B.J. Parman, V. Amanor-Boadu, P.H. Pfromm, Energy 42 (2012) 251.
[19] S.V. Ley, L.A. Paquette, J. Am. Chem. Soc. 96 (1974) 6670.
[20] G.E. Veitch, K.L. Bridgwood, K. Rands-Trevor, S.V. Ley, Synlett (2008) 2597.

[21] C.D. Zeinalipour-Yazdi, J.S.J. Hargreaves, C.R.A. Catlow, J. Phys. Chem. C 119 (2015) 28368.
[22] Y. Abghoui, A.L. Garden, J.G. Howalt, T. Vegge, E. Skúlason, ACS Catal. 6 (2016) 635.
[23] S.J. Henderson, A.L. Hector, J. Solid State Chem. 179 (2006) 3518.
[24] N.E. Brese, M. O'Keeffe, P. Rauch, F.J. DiSalvo, Acta Crystallogr. C 47 (1991) 2291.
[25] S. Royer, D. Duprez, S. Kaliaguine, Catal. Today 112 (2006) 99.
[26] S. Laassiri, N. Bion, D. Duprez, H. Alamdari, S. Royer, Catal. Sci. Technol. 3 (2013) 2259.
[27] Q. Zhang, L. Gao, Langmuir 20 (2004) 9821.
[28] Y. Cong, H.S. Park, H.X. Dang, F.-R.F. Fan, A.J. Bard, C.B. Mullins, Chem. Mater. 24 (2012) 579.
[29] R. Schlögl, Angew. Chem. Int. Ed. 42 (2003) 2004.
[30] O. Lemmermann, Zeitschrift für Pflanzenernährung, Düngung, Bodenkunde 55 (1951) 258.
[31] K. McAulay, J.S.J. Hargreaves, A.R. McFarlane, D.J. Price, N.A. Spencer, N. Bion, F. Can, M. Richard, H.F. Greer, W.Z. Zhou, Catal. Commun. 68 (2015) 53.
[32] R. Kojima, K.-I. Aika, Appl. Cata. A: Gen. 209 (2001) 317.